Highlight Removal in Endoscope Images

Vladimir Bochko; Department of Information Technology, Lappeenranta University of Technology, P. O. Box 20, 53851 Lappeenranta, Finland (botchko@lut.fi)

Yoichi Miyake; Department of Information and Image Sciences, Chiba University, 1-33 Yayoi-cho, Inage-ku, Chiba 263-8522, Japan (miyake@faculty.chiba-u.jp)

Abstract

In this paper, we propose an efficient algorithm for highlight removal in endoscope images. According to the analysis the endoscope images are presented by several kinds of regions and the dichromatic reflection model is not valid for the whole image. However it is possible to segment the image using machine learning algorithms and extract only the body and highlight reflection regions for which the dichromatic reflection model is relevant and then the highlight removal technique is applied. We present the experimental results confirming the method's feasibility.

Introduction

The highlight removal technique reduces the influence of the light source in the highlight region and gives the possibility to see the color of the surface. This improved color reproduction is especially important in medicine in the analysis of endoscope images. An existence of highlights does not prevent doctors making a correct diagnose. However highlights are an undesirable factor when medicine images are merged together to obtain a mosaic image.

There are several proposed approaches of highlight analysis and highlight removal in color images [1-3] and spectral images [4]. They are based on the analysis of body-reflection and highlight clusters. However the algorithms are lacking in sophisticated unsupervised machine learning methods which are efficient and relevant for clustering. The machine learning methods are used in [5, 6] however these studies are based on the dichromatic reflection model while the endoscope images have a more complicated structure.

The highlight removal technique is presented in our previous work [6]. The technique is based on a clustering method that is a mixture of probabilistic principal component analyzers [9], separating all pixels in a spectral domain into body-reflection and highlight reflection clusters, and providing KNN-mapping (k-nearest-neighbors mapping) of the highlight cluster's pixels in the line defined by the direction of the first body-reflection cluster's eigenvector. Though the method's feasibility is demonstrated with spectral images the method has its drawbacks. The method is time and memory demanding due to the use of the KNN algorithm. In addition, the method is not very accurate because KNN-mapping does not provide the correct direction for the projection. It is shown in [2] that the correct mapping for the dichromatic reflection model should be done along the direction which is parallel to the first eigenvector of the highlight cluster. In turn, this direction is parallel to the vector of the light source in the spectral domain.

Our purpose is to generate the image which reproduces the endoscope image where highlight is removed and the color of the object is reproduced instead of highlight. In the next sections we describe the algorithm based on the Gaussian mixture model (GMM) used for clustering and mapping using the illumination vector.

Algorithm

Analysis shows that the data of the endoscope image is represented by highlight, body-reflection and shade regions. The shade regions include a shade of the analyzed object as well as a shade surrounding the highlight region. The last shade occupies a small area. The color of the shade varies significantly in comparison with the background pixels and does not have a smooth transition with the color of the body-reflection cluster. In addition, the clustering algorithms identify the shade as a separate cluster or clusters. This violates the assumption about the dichromatic reflection model. It is supposed in this study that the reflection model is not dichromatic for the entire endoscope image but if only true background and highlight pixels are taken, then the dichromatic reflection model is a realistic assumption.

The algorithm is presented in Algorithm 1. According to the color properties of the endoscope image the algorithm first implements the clustering procedure. If the given number of clusters is two then the algorithm finds the body-reflection and non-body-reflection clusters. The latter includes a highlight and shade. This is because the body-reflection cluster is usually well-defined. It contains the most pixels and represents a compact area of input space. The non-body-reflection cluster cannot directly be used because a mixture of pixels from the shadow and highlight changes the first eigenvector of the highlight cluster and gives an incorrect mapping. The solution is that the algorithm should use the additional pixel clustering procedure for the non-body-reflection cluster. The procedure involves a number of clusters defined by testing the endoscope image. If the number of clusters is small then a part of the shadow recognized as a highlight produces distorted mapping. When the number of clusters is too large then the highlight area is separated into smaller parts and only one of the highlights is removed.

The result of two sequential clustering procedures is the clusters corresponding to the given data set and their parameters. The problem is to decide which two clusters from the cluster set are the body-reflection and highlight clusters. For this, the features of the clusters need to be selected. A feature of the body-reflection cluster is a maximum number of pixels among all clusters or, in other words, a maximum of a prior probability of clusters. A feature of the highlight cluster is a maximum of the norm of the mean vector.

Algorithm 1: The highlight removal algorithm

Input: the observed vector $\mathbf{x} = | x_1, \ldots, x_d |^T$, where d is a dimensionality of data (a number of wavelengths) and T denotes a transposition. For a Gaussian mixture model: a number of clusters for step 2 $M_1 = 2$, a number of clusters for step 4 M_2, and a number of iterations for steps 2 and 4.

Do:

1. Reduce the dimensionality of the input data to three PCs using PCA $\mathbf{x}^{(d)} \rightarrow \mathbf{x}^{(3)} = \mathbf{y}$.
2. Fit the mixture model to the data using the GMM algorithm (M_1) and classify each data point using a maximum of the likelihood $P(\mathbf{y} \mid \varpi_i)$, where ϖ_i denotes an i^{th} cluster ($i = 1,2$)
$$\mathbf{y} \in \begin{cases} \varpi_1 & \text{if } P(\mathbf{y} \mid \varpi_1) \geq P(\mathbf{y} \mid \varpi_2) \\ \varpi_2 & \text{otherwise.} \end{cases}$$
3. Define the body-reflection and non-body-reflection clusters $(\mathbf{y} \mid \varpi_b)$ and $(\mathbf{y} \mid \varpi_n)$, respectively
$$\varpi_b = \begin{cases} \varpi_1 & \text{if } P(\varpi_1) \geq P(\varpi_2) \\ \varpi_2 & \text{otherwise.} \end{cases}$$
4. Fit the mixture model to the samples of the non-body-reflection cluster $(\mathbf{y} \mid \varpi_n)$ using the GMM algorithm (M_2) and classify each data point ($i, j = 1, \ldots, M_2$)
$$\mathbf{y} \in \varpi_{ni} \quad \text{if} P(\mathbf{y} \mid \varpi_{ni}) \geq P(\mathbf{y} \mid \varpi_{nj}), i \neq j.$$
5. Define the highlight cluster $(\mathbf{y} \mid \varpi_h)$, $\overline{\mathbf{y}}$ denotes a mean of $\mathbf{y}$
$$\varpi_h = \varpi_{ni} \quad \text{if} \| \overline{\mathbf{y}} \mid \varpi_{ni} \| > \| \overline{\mathbf{y}} \mid \varpi_{nj} \|, i \neq j.$$
6. Reduce the dimensionality of input data (only pixels of highlight and body-reflection clusters) to the first two PCs using PCA $(\mathbf{x} \mid \varpi_b \varpi_h)^{(d)} \rightarrow (\mathbf{x} \mid \varpi_b \varpi_h)^{(2)} = (\mathbf{z} \mid \varpi_b \varpi_h)$
7. Map each highlight data point of $(\mathbf{z} \mid \varpi_h)$ onto the first eigenvector of the body-reflection cluster $(\mathbf{z} \mid \varpi_b)$ by using the first eigenvector of the highlight reflection cluster.
8. Reconstruct the spectral image and replace only highlight pixels by new ones for the original image.

Reproduce: the spectral image with a synthetic part instead of a highlight region in a suitable color system (e.g. RGB CIE 1931).

The algorithm is implemented the following steps. In step 1 PCA is used to reduce the data dimensionality and to obtain three principal components (PCs). This number of PCs for endoscope images is suggested in [8]. In step 2 the GMM algorithm [7, 9] is applied to find the clusters in the space spanned by three eigenvectors. Only two clusters are utilized by the algorithm in step 2 and the body-reflection cluster is one of them. This cluster is characterized by the most pixels. Therefore, the largest value of the prior probability after using the GMM algorithm characterizes the body-reflection cluster (step 3). In step 4 the algorithm separates the non-body-reflection cluster into several smaller ones and only one of them, which has the maximum norm of the mean vector, is a highlight cluster (step 5). After the clustering procedure, pixels belonging to the highlight and body-reflection clusters are marked by labels. Therefore, highlight and body-reflection pixels are known for their input space and its subspaces.

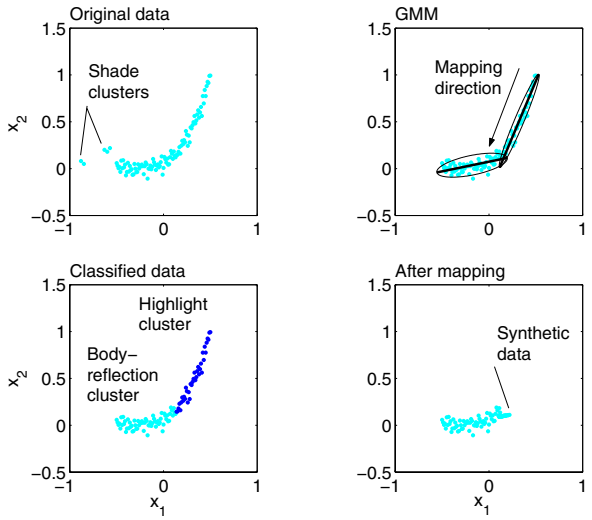

Figure 1. The illustration of the algorithm work with a synthetic dataset. Initially the data contains highlight, body-reflection and shade clusters. After classification only body-reflection and highlight clusters are considered. The Gaussian mixture model fits the data, and the first eigenvector of the highlight cluster is used as a mapping direction for the highlight pixels. The pixels are mapped onto the line defined by the first eigenvector of the body-reflection cluster (a synthetic data in right bottom figure). Note: shade pixels and pixels of body-reflection are kept untouched and reproduced as they are.

Owing to the fact that the body and surface reflection pixels satisfying the dichromatic reflection model lie on the plane, the PCA is used once more to reduce the dimensionality of input data (highlight and body-reflection pixels) and to obtain two PCs (step 6). The clustering results obtained in three-dimensional space are used for the dichromatic plane. The correct projection is found by using the intersection dot between two lines defined by two dots each. The dots of the first line are determined by the mean value and the sum of the mean value and the first eigenvector of the body-reflection cluster. The second line is defined by the value of the pixel being projected and the sum of the same pixel value and the first eigenvector of the highlight cluster. Finally, highlight pixel mapping is done in the direction parallel to the first eigenvector of the highlight cluster. The pixels are mapped in the line defined by the direction of the first eigenvector of the body-reflection cluster (step 7). Fig. 1 illustrates the mapping procedure.

We will refer to the algorithm based on KNN-mapping the KNN algorithm [6] and the algorithm based on the mapping using the illumination vector the IM algorithm. Algorithm 1 represents the IM algorithm.

The IM algorithm is fast due to the following reasons. The clustering procedure is implemented in three-dimensional space while the input space is 61-dimensional. The GMM algorithm finds two clusters for many samples in a very fast way. The GMM algorithm is also fast for

separating a reduced number of samples (the non-body-reflection cluster) into several clusters. KNN-mapping is excluded. In addition, the algorithm does not require significant memory space.

The good accuracy of the algorithm is provided by mapping in a two-dimensional space based on body- and highlight reflection clusters found in three-dimensional space (clustering in the two-dimensional space reduces accuracy because the dichromatic reflection model is not suitable). In addition, the mapping incorporates the illumination vector's direction.

Experiment

The experiment was conducted with a real endoscope image obtained by using a spectral endoscope [10]. The image size is 640x480 pixels and the spectral dimension is presented by 61 components taken evenly in the range 400-700nm.

To provide fast work only image parts were used in analysis and then after highlight removing they were embedded in the whole image. This was also needed because the common model does not correspond to the dichromatic reflection model. This is due to the spotty shade including the varied colors nearby with the highlight regions. Thus, to reduce color variations it is better to work with a smaller region than with a whole image. This also helps to avoid multiple highlights due to variations of the analyzed object shape [5]. However, multiple highlights are possible if the background pixels have a restricted change of intensity (for example, the regions shown in Fig. 3 and Fig. 5). It is assumed that the dichromatic reflection model is still valid for body-reflection and highlight regions (without shade).

Fig. 3 shows the result for the image part where KNN and IM algorithms were used. The image size is 81x81 and 61 components. The KNN algorithm does not work with the images of the larger size because it would need a larger memory space. Twenty iterations were used and two Gaussians were initially given for the GMM method used in the IM algorithm. After this, the non-body-reflection cluster was separated by using the GMM with 30 iterations and 4 Gaussians ($M_2 = 4$). These parameters were determined experimentally. The same parameters were adjusted for the IM algorithm in all tests.

The computational time for the image region shown in Fig. 3 is presented in Table 1 (Matlab 6.5, Intel Pentium III Processor, 800 MHz, 512 MB of RAM).

Table 1: The computational time (s)

KNN	IM
304.62	12.81

Fig. 4 shows the highlight region (the spectral image region size is 41x41 pixels and 61 components) from the bottom part of the endoscope image and the result of the highlight removal by the IM algorithm. Table 2 shows the priors and norms of the means for the Gaussian mixture model for the image shown in Fig. 4. In Table 2 and Table 3 the priors in the second column are given for step 2 of the algorithm, where separation was done for two clusters. The third and fourth columns of Table 2 and Table 3 show the priors and norms for step 4 of the algorithm where four clusters were used.

Table 2: The trained model priors and norms (the IM algorithm)

Clusters	Priors	Priors	Norms
1	0.0986	0.2450	3.8372
2	0.9014	0.1919	6.9679
3		0.1905	2.2079
4		0.3726	4.8449

Table 2 illustrates that the IM algorithm extracts features of the body-reflection and highlight clusters. This can be clearly seen from the prior probability values and the maximum norm of the mean. The computational time for the image region shown in Fig. 4 is 3.11 s. The chromaticity histogram for this region is shown in Fig. 2.

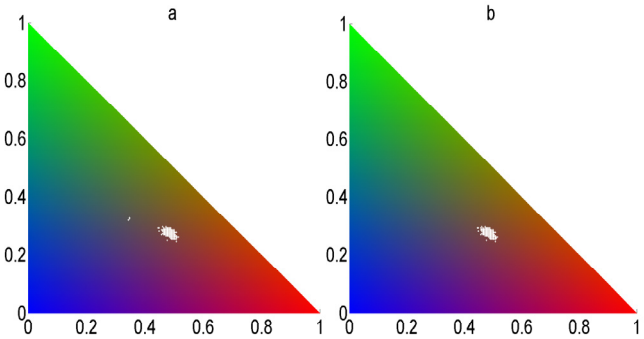

Figure 2. a) A chromaticity histogram for the region shown in Fig. 4 (left). b) A chromaticity histogram for the region shown in Fig. 4 (right). The highlight dots are seen nearby with the center of the color diagram in Fig. 2.a. They are not seen after highlight removal (Fig. 2.b). The chromaticity diagram coordinates are r (horizontal) and g (vertical).

Fig. 5 shows many highlight regions from the central part of the endoscope image. The size of the spectral image region is 111x101 pixels and 61 spectral components. Table 3 shows the priors and norms of the means for the Gaussian mixture model for the image shown in Fig. 5.

Table 3: The trained model priors and norms (the IM algorithm)

Clusters	Priors	Priors	Norms
1	0.0484	0.2851	6.1118
2	0.9516	0.0850	4.5245
3		0.4929	5.0451
4		0.1369	5.5221

From Table 3 (column 2) one can see that one cluster has a prior value that is significantly greater than the other. This determines the feature of the body-reflection cluster. At the same time only one mean vector in the space spanned by three eigenvectors has a norm value that is greater than the others (Table 3, column 4). Hence, the informative feature for the highlight cluster is the norm of its mean vector. The computational time for the image region shown in Fig. 5 is 25.84 s.

Finally, the regions with removed highlight shown in Fig. 4 and Fig. 5 replace the corresponding regions in the whole endoscope image (Fig. 6 and Fig. 7).

The experimental results demonstrate that the IM algorithm removes highlight in the regions of the test image. The IM algorithm, less computationally demanding in comparison with the KNN algorithm, provides better color reproduction replacing a highlight. Further research can be done to improve the used features of clusters. For example, this can be done for the image in Fig. 5 where the highlight features of several clusters have close values (Table 3).

Conclusion

It was shown in this study that while body-reflection and highlight reflection can be described by the dichromatic reflection model in endoscope images, the existence of the spotty shade including pixels with different colors destroys an assumption about the model and makes the task of highlight removal difficult.

The proposed algorithm, based on machine learning, removes highlight in the endoscope image and improves color reproduction of the entire image.

There is no quantitative measure of quality for highlight removal. The technique also depends on data that affects the algorithm's performance. However, it is supposed that the considered method can be useful in medical applications where mosaic images are required.

Acknowledgements

The authors thank the Academy of Finland for the funding granted to this study and Prof. T. Igarashi for suggestions on the use of highlight removal techniques in medicine.

Figure 3. From left to right: RGB-representation of the original image, the result of the KNN and IM algorithms, respectively.

Figure 4. From left to right: RGB-representation of the original image, the result of the IM algorithm.

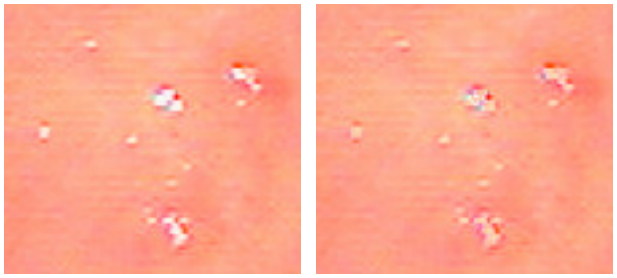

Figure 5. From left to right: RGB-representation of the original image, the result of the IM algorithm.

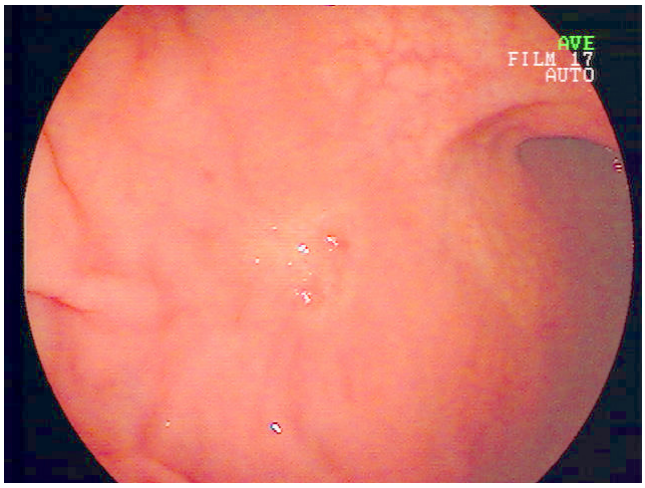

Figure 6. RGB-representation of the original endoscope image.

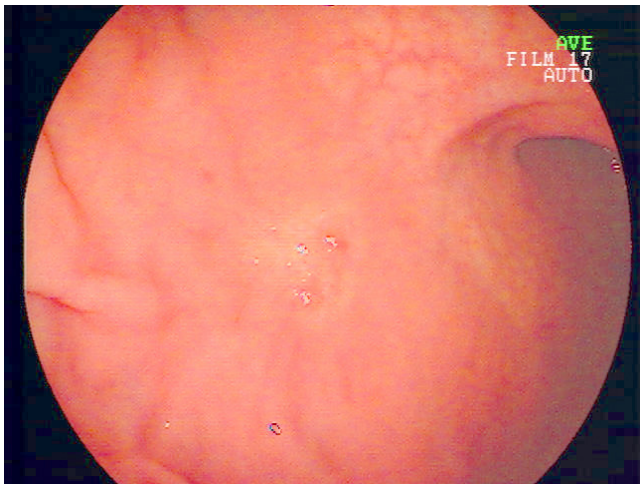

Figure 7. RGB-representation of the spectral image with removed highlight by the IM algorithm.

References

[1] A. Hanbury, Highlight Detection by 2D-Histogram Analysis, Proc. SGIV, Aachen, Germany, pp. 167-172. (2004).

[2] K. Schluns and A. Koschan, Global and Local Highlight Analysis in Color Images, Proc. CGIP, Saint-Etienne, France, pp. 300-304. (2000).

[3] F. Tong and B. V. Funt, Specularity Removal for Shape from Shading, Proc. Vision Interface Conf., Edmonton, AB, Canada, pp. 98-103. (1988).

[4] S. Tominaga, E. Takahashi, and N. Tanaka, Parameter Estimation of a Reflection Model from a Multiband Image, Proc. IEEE Workshop on Photometric Modeling for Computer Vision and Graphics, Los Alamitos, Calif., pp. 56-63. (1999).

[5] H. J. Andersen and M. Storring, Classifying Body and Surface Reflections Using Expectation-Maximization, Proc. PICS, Rochester, New York, pp. 441-446. (2003).

[6] V. Bochko and J. Parkkinen, Highlight Analysis Using a Mixture Model of Probabilistic PCA, WSEAS Trans. On Systems, Vol. 4, Is. 1, pp. 55-59. (2005).

[7] I. T. Nabney, Netlab Algorithms for Pattern Recognition (Springer, 2002).

[8] T. Shiobara, S. Zhou, H. Haneishi, N. Tsumura and Y. Miyake, Improved Color Reproduction of Electronic Endoscopes, J. Imaging Sci. and Technol., Vol. 40, No 6, pp. 494 – 501. (1996).

[9] M. E. Tipping and C. M. Bishop, Mixtures of Probabilistic Principal Component Analyzers, Neural Computation, Vol. 11, No. 2, pp. 443-482. (1999).
[10] Y. Miyake, T. Kouzu, S. Takeuchi, S. Yamataka, T. Nakaguchi and N. Tsumura, Development of New Electronic Endoscopes Using the Spectral Images of an Internal Organ, Proc. CIC, Scottsdale, Arizona, pp. 261-263. (2005).

Author Biographies

Vladimir Bochko is a Docent at the Department of Information Technology, Lappeenranta University of Technology. He is a member of the Finnish Pattern Recognition Society.

Yoichi Miyake is a Professor at the Department of Information and Image Sciences, Chiba University. He has published more than 200 original papers and 18 books in the field of color image processing, analysis and evaluation. He is a pioneer in multispectral imaging research.